An investigation of the spectral structure of atmospheric waves near a jet stream

By CHING-YEN TSAY[1] and S. K. KAO, *Department of Meteorology, University of Utah, Salt Lake City, Utah, USA*

(Manuscript received August 7; revised version October 30, 1972)

ABSTRACT

An investigation of the nonlinear interaction near the center of maximum mean motion of a jet stream indicates that interactions of waves of low frequencies and those between the mean zonal motion and low frequency waves contribute most to the low frequency range of the energy spectrum of the zonal component of the turbulent motion, whereas the effects of the sphericity and Reynolds stresses contribute most to the low frequency range of the spectra of the meridional turbulent motion. In ranges of intermediate and high frequencies, the interactions between the mean zonal motion and waves of frequency range in question contribute most to the respective spectra. In the investigation of the spectral structure of atmospheric waves near a jet stream, it is found that in the region of the maximum zonal mean motion the kinetic energy of the zonal and meridional components of the turbulent motion is generally contributed by the nonlinear interactions between waves of various frequencies with the mean zonal motion. It is also found that as waves travel eastward from the center of maximum mean zonal motion, the velocity-amplitudes of waves of low frequencies grow at the expense of the kinetic energy of waves of higher frequencies. This suggests that center maximum mean motion of the jet stream tends to excite wave motion of high frequencies, and that the kinetic energy of these waves is transferred to waves of lower frequencies through nonlinear interactions.

I. Introduction

One of the fruitful lines of studying wave motion in the free atmosphere is the analysis of the power and cross spectra of the motion. In recent years, analyses have been made on wave number spectra (Benton & Kahn, 1958; Saltzman, 1958; Saltzman & Fleishman, 1962; Eliasen, 1958; Eliasen & Machenhauer, 1965, 1969; Barrett, 1961; Van Mieghem, 1961; Kao, 1954) on Eulerian-frequency spectra (Estoque, 1955; Van der Hoven, 1958; Chiu, 1961, 1968; Kao & Bullock, 1964; Kao, 1965), on Lagrangian frequency spectra (Kao, 1962; Kao & Bullock, 1964; Kao, 1965; Kao & Gain, 1968; Kao & Powell, 1969; Kao & Henderson, 1970) and on wave number-fre-quency spectra (Kao, 1968; Kao & Wendell, 1970; Kao, Tsay & Wendell, 1970; Kao & Sagendorf, 1970). These studies have contributed a great deal to the understanding of characteristics of wave motions in the free atmosphere.

The objectives of this study are three-fold: an analysis of the Eulerian-frequency spectra, a study of wave interactions at various locations in the middle latitudes of the northern hemisphere, and an investigation of the effect of a jet stream on the spectral structure of atmospheric waves in the middle latitude.

Studies of the effect of jet streams on the hydrodynamic stability of atmospheric waves have been made by Kuo (1961) and Lipps (1963). These authors were primarily interested in the effect of the mean motion of a jet current on the development of waves. Therefore, the effect of nonlinear interactions between waves of various scales was not taken into account. It is known that the mean motion affects wave motion most at the incipient stage of the development, and that in the course of development the effect of nonlinear interactions becomes important. One of the objectives of this study is to investigate how the wave interactions

[1] Present affiliation: National Center for Atmospheric Research, Boulder, Colorado.

would affect the development of atmospheric waves near a jet stream. To accomplish this goal, spectral analyses are made a number of locations along a latitudinal circle passing through the center of the maximum mean motion, then the structure of the waves at various stages of the development is investigated.

II. Theoretical background

2.1. *Transform and spectrum in frequency domain*

We consider an atmospheric quantity with the real single-valued function $q(\lambda, \phi, p, t')$ where λ, ϕ, p and t' stand for longitude, latitude, pressure, and time. Since in this study longitudes, latitudes, and pressure levels are considered as parameters, we shall, for brevity, denote the function at a certain longitude, latitude, and pressure level in the atmosphere by $q(t')$. If the function has a finite number of finite discontinuities over a period of time T, which is normalized to 2π, $q(t)$ is piecewise differentiable in the domain $0 \leqslant t \leqslant 2\pi$, where $t = (2\pi/T)t'$. Under these conditions $q(t)$ may be transformed into a frequency space.

The Fourier transform[1] and their inverse transform are as follows:

$$Q(n) = \frac{1}{2\pi}\int_0^{2\pi} q(t)e^{-int}\,dt \qquad (2\text{-}1)$$

$$q(t) = \int_{-\infty}^{\infty} Q(n)e^{int}\,dn \qquad (2\text{-}2)$$

where n represents nondimensional frequency, $n = T/2\pi$ (frequency).

For convenience of computations in this study we express

$$Q(n) = Q_r(n) + i\,Q_i(n) \qquad (2\text{-}3)$$

where

$$Q_r(n) = \frac{1}{2\pi}\int_0^{2\pi} q(t)\cos nt\,dt \qquad (2\text{-}4)$$

and

$$Q_i(n) = -\frac{1}{2\pi}\int_0^{2\pi} q(t)\sin nt\,dt \qquad (2\text{-}5)$$

are the real and imaginary parts, respectively, of $Q(n)$.

Considering another scalar function $h(t)$ with a Fourier transform $H(n)$ it can be shown that

$$\frac{1}{2\pi}\int_0^{2\pi} q(t)\,h(t)\,e^{-int}\,dt = \int_{-\infty}^{\infty} Q(m)\,H(n-m)\,dm = \int_{-\infty}^{\infty} Q(n-m)\,H(m)\,dm \qquad (2\text{-}6)$$

Let, $n \to 0$, eq. (2-6) gives

$$\frac{1}{2\pi}\int_0^{2\pi} q(t)\,h(t)\,dt = \int_{-\infty}^{\infty} Q(m)\,H(-m)\,dm = \int_{-\infty}^{\infty} Q(n)\,H(-n)\,dn = \int_{-\infty}^{\infty} Q(-m)\,H(m)\,dm = \int_{-\infty}^{\infty} Q(-n)\,H(n)\,dn \qquad (2\text{-}7)$$

Let $q(t) = h(t)$, then $Q(n) = H(n)$, and we have the transform formula for the variance of q expressed in relation to the power spectrum

$$\frac{1}{2\pi}\int_0^{2\pi} q^2(t)\,dt = \int_{-\infty}^{\infty} |Q(n)|^2\,dn \qquad (2\text{-}8)$$

Eqs. (2–7) and (2–8) enable us to define the cross and power spectrum as follows:

$$E_{qh}(n) = 2Q(n)\,H(-n) = 2Q(-n)\,H(n), \quad E_{qh}(0) = Q(0)\,H(0) \qquad (2\text{-}9)$$

$$E_{\frac{1}{2}q^2}(n) = |Q(n)|^2 \equiv EQQ(n), \quad E_{\frac{1}{2}q^2}(0) = \tfrac{1}{2}|Q(0)|^2 \equiv EQQ(0) \qquad (2\text{-}10)$$

2.3. *Linear and nonlinear interaction in frequency domain*

In the longitude, latitude, pressure coordinate system, the equations of horizontal motion on the isobaric surface are

[1] It may be remarked that there are many ways of calculating a frequency spectrum. The reason for employing Fourier analysis is that it provides a consistent procedure for the analysis of nonlinear interaction as shown in a later section of this paper.

$$\frac{\partial u}{\partial t'} = -\left(\frac{1}{a\cos\phi}uu_\lambda + \frac{1}{a}vu_\phi + wu_p - \frac{\tan\phi}{a}vu\right) + fv - \frac{g}{a\cos\phi}Z_\lambda + F_1 \quad (2\text{-}11)$$

$$\frac{\partial v}{\partial t'} = -\left(\frac{1}{a\cos\phi}uv_\lambda + \frac{1}{a}vv_\phi + wv_p + \frac{\tan\phi}{a}uu\right) - fu - \frac{g}{a}Z_\phi + F_2 \quad (2\text{-}12)$$

where λ, ϕ, and p denote the longitude, latitude, and pressure coordinates, respectively, the subscripts indicate differentiation, t is time, u and v the longitudinal and meridional component of the velocity, respectively, w the individual rate of change of pressure, a radius of the earth, f the Coriolis parameter, g the acceleration of gravity, Z the height of an isobaric surface, and F_1 and F_2 the longitudinal and latitudinal components of the combined molecular and Reynolds stress forces due to motions of scale smaller than that in question.

Deriving the energy equation in frequency domain, the following notations for the transforms, as defined by (2-1) and (2-3), will be used

$q(t;p,\lambda,\phi)$	u	v	w	u_g	v_g	F_1	F_2
$Q(n;p,\lambda,\phi)$	U	V	W	UG	VG	G_1	G_2

where u_g and v_g are the longitudinal and latitudinal components of the geostrophic wind with

$$v_g = \frac{g}{f}\frac{1}{a\cos\phi}Z_\lambda \quad (2\text{-}13)$$

$$u_g = -\frac{g}{f}\frac{1}{a}Z_\phi \quad (2\text{-}14)$$

Since $t' = \frac{T}{2\pi}t, \frac{\partial u}{\partial t'} = \frac{2\pi}{T}\frac{\partial u}{\partial t}$.

Fourier transform of (2-11) and (2-12) gives

$$\frac{2\pi}{T}\,\mathrm{in}\;U(n) = -\int_{-\infty}^{\infty} dm\left[\frac{1}{a\cos\phi}U(n-m)\,U_\lambda(m) + \frac{1}{a}V(n-m)\,U_\phi(m) + W(n-m) \times U_p(m) - \frac{\tan\phi}{a}V(n-m)\,U(m)\right] + f[V(n) - VG(n)] + G_1(n) \quad (2\text{-}15)$$

$$\frac{2\pi}{T}\,\mathrm{in}\;V(n) = -\int_{-\infty}^{\infty} dm\left[\frac{1}{a\cos\phi}U(n-m)\,V_\lambda(m) + \frac{1}{a}V(n-m)\,V_\phi(m) + W(n-m) \times V_p(m) + \frac{\tan\phi}{a}U(n-m)\,U(m)\right] - f[U(n) - UG(n)] + G_2(n) \quad (2\text{-}16)$$

Multiplication of (2-15) and $\{(T/2\pi)(1/in)\times U(-n)\}$ gives the energy equation of zonal component in frequency domain

$$E_{u^2/2}(n) = -\frac{T}{2\pi}\frac{i}{n}\left\{-\int_{-\infty}^{\infty} dm\,U(-n) \times\left[\frac{1}{a\cos\phi}U(n-m)\,U_\lambda(m) + \frac{1}{a}V(n-m)\,U_\phi(m) + W(n-m)\,U_p(m) - \frac{\tan\phi}{a}V(n-m)\,U(m)\right] + f\,U(-n) \times[V(n) - VG(n)] + U(-n)G_1(n)\right\} \quad (2\text{-}17)$$

Similarly, multiplication of (2-16) and $\{(T/2\pi)\times(1/in)\,V(-n)\}$ gives the energy equation of meridional component in frequency domain.

$$E_{v^2/2}(n) = -\frac{T}{2}\frac{i}{n}\left\{-\int_{-\infty}^{\infty} dm\,V(-n) \times\left[\frac{1}{a\cos\phi}U(n-m)\,V_\lambda(m) + \frac{1}{a}V(n-m)\,V_\phi(m) + W(n-m\;V_p(m) + \frac{\tan\phi}{a}U(n-m)\,U(m)\right] - f\,V(-n) \times[U(n) - UG(n)] + V(-n)\,G_2(n)\right\} \quad (2\text{-}18)$$

Eqs. (2-17) and (2-18) will be used for the analysis of nonlinear interactions of the large scale waves near a jet stream.

III. Data and computations

3.1. *Source and type of data*

The data used in this study were obtained from the 12-hourly 500 mb height and stream function analyses of the National Meteorological Center. The values of height and stream function were available over the portion of the Northern Hemisphere north of 17.5° N. latitude on the NMC octagonal grid with a grid interval of 381 km. The period from 0000Z 1 December 1963 through 0000Z 1 December 1964 was selected because the data available for this year was far more complete than the data available for other periods.

The stream function data were computed at the NMC through a finite difference solution of the balance equation

$$\nabla^2\psi = \frac{1}{f}\left\{\nabla^2\Phi + 2\left[\left(\frac{\partial^2\psi}{\partial x\,\partial y}\right)^2 - \frac{\partial^2\psi}{\partial x^2}\frac{\partial^2\psi}{\partial y^2}\right] - \nabla\psi\,\nabla f\right\} \tag{3-1}$$

where f is the Coriolis force, Φ is the geopotential height of a pressure surface and ψ is the stream function. The balance equation is obtained by first taking the divergence of the equation of motion for nonviscous flow and then setting the divergence and its total derivative equal to zero. This permits us to define the stream function derived winds with

$$\mathbf{V} = \mathbf{k} \times \nabla\psi \tag{3-2}$$

where $\mathbf{k}$ represents the unit vector in the zenith direction.

The addition of divergent portion of the wind would make the study more realistic, but the velocity potential analyses was not immediately available. However, since this analysis is made at 500 mb, which is close to the level of nondivergence, the use of the nondivergence wind should be reasonable (Charney, 1948).

3.2. *Computational form of kinetic energy equations*

The wind data used in this study are derived from the stream function, and therefore represent only the horizontal part of motion. Furthermore, the vertical velocity resulting from the large-scale atmospheric motion is generally much smaller than horizontal motion (Phillips, 1963). Thus, for the computations involved in this work, the terms involving vertical velocity are neglected, and the energy equations (2-17) and (2-18) may be expressed

$$\begin{aligned} EUU(n) = \frac{T}{2\pi}\Big\{ & \underset{(\mathrm{U1})}{U(-n)\frac{i}{na\cos\phi}\sum_m U(n-m)\,U_\lambda(m)} \\ & + \underset{(\mathrm{U2})}{U(-n)\frac{i}{na}\sum_m V(n-m)\,U_\phi(m)} \\ & - \underset{(\mathrm{U3})}{U(-n)\,i\frac{\tan\phi}{na}\sum_m V(n-m)\,U(m)} \\ & - \underset{(\mathrm{U4})}{U(-n)\frac{i}{n}f[V(n)-VG(n)]} \\ & - \underset{(\mathrm{U5})}{\frac{i}{n}U(-n)\,G_1(n)}\Big\} \end{aligned} \tag{3-3}$$

$$\begin{aligned} EVV(n) = \frac{T}{2\pi}\Big\{ & \underset{(\mathrm{V1})}{V(-n)\frac{i}{na\cos\phi}\sum_m U(n-m)\,V_\lambda(m)} \\ & + \underset{(\mathrm{V2})}{V(-n)\frac{i}{na}\sum_m V(n-m)\,V_\phi(m)} \\ & + \underset{(\mathrm{V3})}{V(-n)\,i\frac{\tan\phi}{na}\sum_m U(n-m)\,U(m)} \\ & + \underset{(\mathrm{V4})}{V(-n)\frac{i}{n}f[U(n)-UG(n)]} \\ & - \underset{(\mathrm{V5})}{\frac{i}{n}V(-n)\,G_2(n)}\Big\} \end{aligned} \tag{3-4}$$

The symbols below the terms on the right side of the equations are for future reference. The

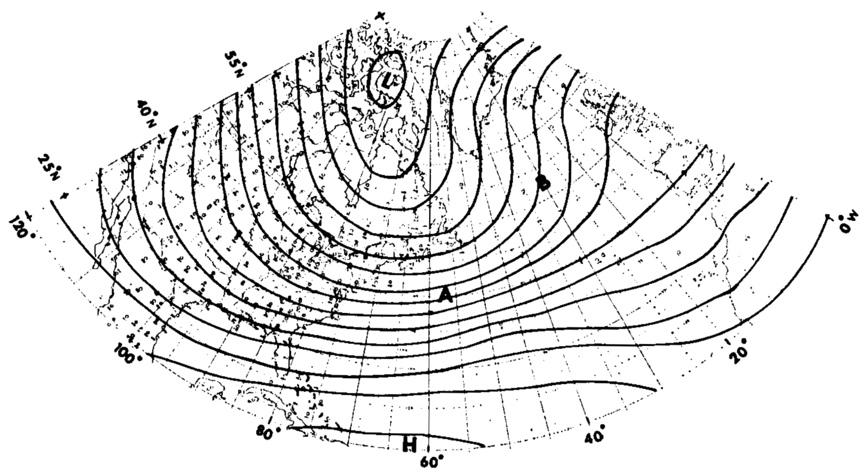

Fig. 1. The distribution of average stream function in winter 1964.

summations over m are from $-m_s$ to m_s, where m_s depends on the number of discrete time data points used; $m_s = 90$ cycles/(90 days) in this study. Summation is used here in place of integration with respect to m, as in equations (2-17) and (2-18), because the transforms are computed for integral values of frequency. This is equivalent to assuming $q(t)$ to be periodic over the time period selected for the analysis.

The interaction terms involving derivatives with respect to longitude and latitude are computed by a centered difference with $\Delta\lambda = 10°$ and $\Delta\phi = 5°$.

IV. Distributions of the mean stream function and kinetic energy of mean and turbulent motion

To provide a framework for the analysis of the effect of a jet stream on the spectral structure of atmospheric waves, the distribution of the mean stream function for winter 1964 in the region, 20° N to 80° N and 0° W to 120° W, which covers the American continent and the Atlantic Ocean, is plotted in Fig. 1. In this figure, letters A and B represent the center of maximum kinetic energy for mean and turbu-

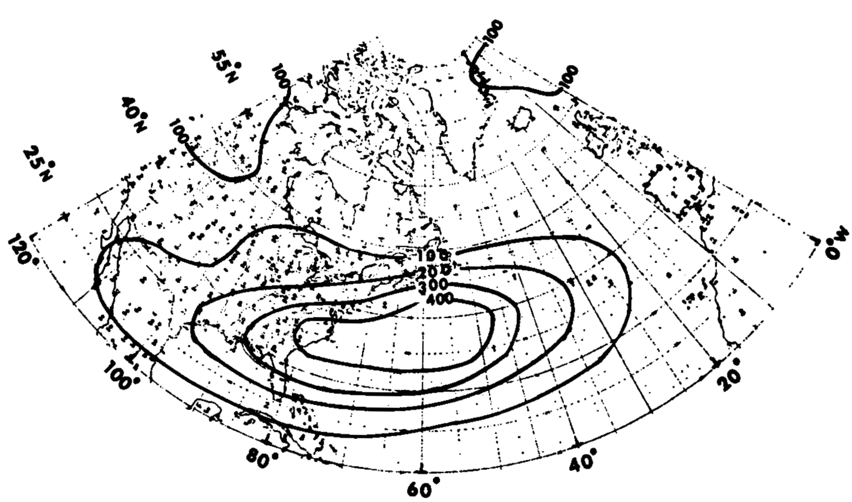

Fig. 2a. The distribution of the kinetic energy for zonal mean motion, $\frac{1}{2}\bar{U}^2$, in 10^4 cm^2 sec^{-2}, winter 1964.

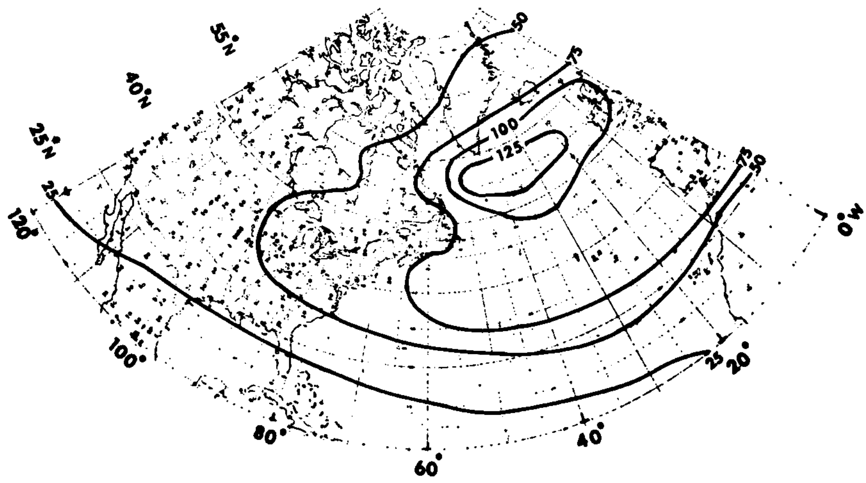

Fig. 2b. The distribution of the average kinetic energy for zonal turbulent motion, $\frac{1}{2}\overline{u'^2}$, in 10^4 cm^2 sec^{-2}, winter 1964.

lent motion, respectively. It is observed that a high stream function center occurred near 20° N, 65° W, and a low center was located at 70° N, 80° W. The center of maximum kinetic energy of mean motion was located at 40° N, 60° W whereas a center of maximum kinetic energy of turbulent motion occurred in the region 50° N to 55° N and 20° W to 40° W. The northeast displacement of turbulent kinetic energy from the center of maximum kinetic energy of mean motion has also been observed by Kao & Hurley (1962).

The distributions of kinetic energy of mean and turbulent motion are plotted separately for zonal and meridional components in Figs. 2 and 3. The maximum of kinetic energy of zonal component occurred between 40° W and 80° W near 40° N, while that of the meridional component occurred between 40° W and 20° W near 50° N. The kinetic energy of the turbulent mo-

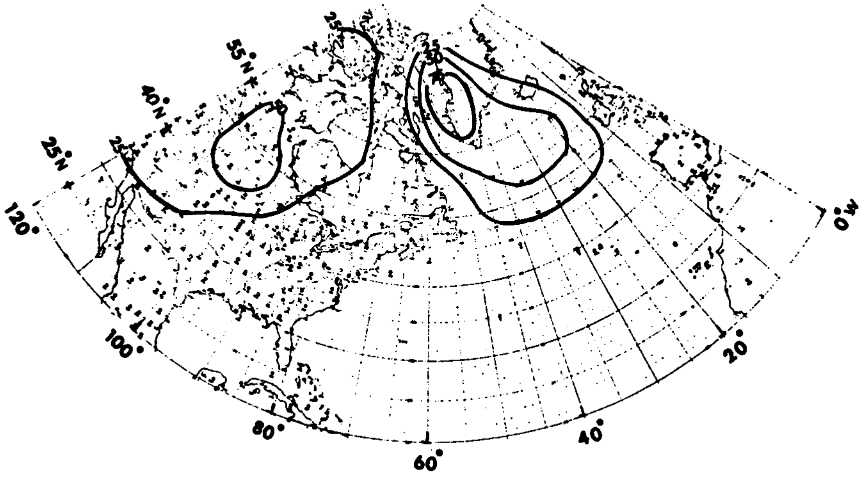

Fig. 3a. The distribution of the kinetic energy for meridional mean motion, $\frac{1}{2}\bar{V}^2$, in 10^4 cm^2 sec^{-2}, winter 1964.

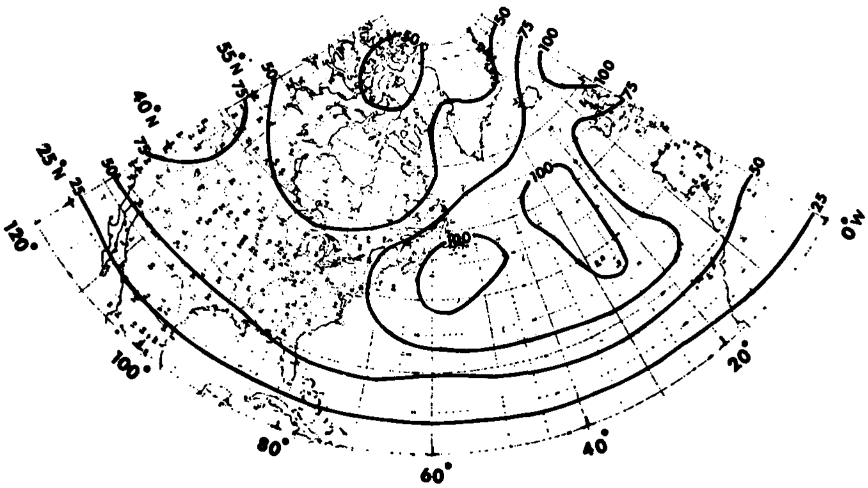

Fig. 3b. The distribution of the average kinetic energy for meridional turbulent motion, $\frac{1}{2}\overline{v'^2}$, in 10^4 cm^2 sec^{-2}, winter 1964.

tion of both components shows higher value to the east of 80° W on 40° and 55° N with maximum located between 20° and 40° W near 55° N for the zonal velocity and between 40° and 60° W near 40° N for the meridional velocity.

V. The linear and nonlinear interactions

5.1. *General discussion*

The nonlinear interaction terms U1, U2, U3 in eq. (3-3) and V1, V2, V3 in eq. (3-4) involve sums of products of transforms for various frequencies in the form

$$\sum_{m=-m_s}^{m_s} Q(n-m)\,P(m).$$

It may be noted from these terms that, depending on the values of n, each term involves from 91 to 180 products of Fourier coefficients. Each product may be considered and interaction between a wave of complex amplitude Q, frequency $(n-m)$ an a wave of complex amplitude P, frequency m. For simplicity, we will say that $(n-m)$ interacts with m. If m is allowed to vary over its entire range, the terms U1, U2, U3 and V1, V2, V3 represent the total contributions from all possible interactions. It may be noted that both $(n-m)$ and m could be negative. However, it can be shown (Appendix A) that the interaction of two given waves of frequencies k and j (if $k>j$) with their complex amplitude $Q(k)$ and $P(j)$ would result in two waves: one with frequency $k+j$, and with complex amplitude $Q(k)\ P(j)$, and the other with frequency $k-j$, and with complex amplitude $Q(k)\,P(-j)$. Therefore, the negative values of m (or $n-m$) represent the interaction of $|m|$ (or $|n-m|$) and $n-m$ (or m) and contribute to the frequency n with the amplitude $Q(|n-m|)$ $P(-|m|)$ or $Q(-|n-m|)P(|m|)$. Since the interaction of waves of frequencies k and j results in two waves of frequencies $k+j$ and $k-j$, we will say k interacts with j and k interacts with $-j$ to distinguish them.

For the convenience of presentation, we classify the frequency range into stationary ($n=0$), low frequency range ($n=1$ to 10, i.e., period 9 to 90 days), intermediate frequency range ($n=11$ to 30, i.e., period 3 to 9 days), and high

Table 1. *Partition classification according to frequency*

Frequency, n, (cycles/ 90 days)	Period, p, (days)	Definition (frequency)	Symbol
0		Zero	0
1 to 10	9 to 90	Low	L
11 to 30	3 to 9	Intermediate	I
31 to 90	1 to 3	High	H

frequency range ($n = 31$ to 90, i.e., period 1 to 3 days), as shown in Table 1. Since we use the negative frequencies, this classification contains 7 frequency categories. The interactions are designated by placing the frequency category symbols side by side with an asterisk separating them, for example, interaction between stationary and low frequency waves is denoted by 0 * L.

Those terms in energy eqs. (3-3) and (3-4) are computed for the separate frequencies of each category. The results for each frequency are then summed over each category and presented in block diagram form, as shown in Figs. 4–9. In these figures, the total contributions of each of the terms in (3-3) and (3-4) are shown in the small blocks in the center of the diagram and labeled with the symbols for the terms they represent. The terms U1 and V1 represent the nonlinear interaction due to the zonal advection of the zonal and meridional components of kinetic energy, U2 and V2 the nonlinear interaction due to the meridional advection of the zonal and meridional components of kinetic energy, U3 and V3 the effect of the earth's curvature, U4 and V4 the effect of ageostrophic winds. The ageostrophic terms represent contributions to the energy through the rate of work done by the pressure and Coriolis forces. They do not involve nonlinear interactions. All of the above terms are computed directly from the available pressure and wind data. The terms U5 and V5, however, cannot be computed directly because no data concerning the eddy stresses force of subgrid scales is available. The sums of the quantities U1 through U4 and V1 through V4 are displayed below the appropriate blocks. To the left of these sums are shown the sums of the spectral energy over the category. The difference between these two terms are displayed to the right and labeled $U5 + E_1$ and $V5 + E_2$. These quantities contain, in addition to the subgrid eddy stresses, the results of error in the data and computational error. The large blocks, connected with arrows to the small blocks labeled U1, U2, V1, and V2, contain positive and negative interactions contributing to the small blocks. A negative value for an interaction combination is interpreted as extractions to the spectral energy. Positive values are interpreted as contributions to the spectral energy. The figures at the bottom of the large blocks represent the total positive and negative contributions from all the interaction combinations.

The interaction computations have been made at the locations, 0°, 20°, 40°, 60°, 80°, 100°, and 120° W on 40° N for 500 mb, winter 1964 (Tsay, 1972). We will only discuss the results at the locations near the jet stream (60° and 40° W on 40° N).

5.2. *The nonlinear interactions at locations near the jet Stream (60° and 40° W on 40° N)*

(*a*) *Low frequency category, L* (*Figs. 4 and 5*). Near the center of the maximum mean velocity at 60° W, U1 is the largest interaction term for the zonal component of energy equation. It contains several interaction combinations of the same order of magnitude: L * –L, 0 * L, and –L * L. The variability of the sign of interactions in U2 causes it to appear smaller as compared with U1. The major interaction combinations for U2 involve positive L * 0, –I * I, H * –I and negative I * –I, I * L. The term U3 gives a positive contribution. The ageostrophic term, U4, and the friction plus error term tend to counteract the large positive contributions through U1. For the meridional component of energy, V3 is the major interaction term. The small value of V1 is due to the cancellation of large positive interactions (L * 0, –L * L, I * –I, H * –H) and negative interactions (0 * L). The term V2 has large negative value because of the negative interactions of –H * H, 0 * L, H * –H, and –I * I. The eddy friction plus error term give positive contribution, while the ageostrophic term serves to extract energy from the low frequency waves.

To the east of the center of maximum velocity at 40° N, U2 and V2 are the most significant interaction terms. Both U2 and V2 contain several interaction combinations of the same order of magnitude: positive L * –L, –L * L, I * –L, –H * H and negative –I * I for U2 and positive –L * L, L * –L and negative –I * I for V2. Both U2 and V2 extract energy. –L * L and L * –L are the major negative interaction combinations for U2, while 0 * L is for V2. The ageostrophic terms U4 and V4 give negative contributions, while U3, V3, and $U5 + E_1$, $V5 + E_2$ give positive contributions.

(*b*) *Intermediate frequency category, I* (*Figs. 6 and 7*). At both locations (60° W and 40° W on 40° N) the interaction terms U1 and V1, contributing to this category, are by far the largest

L (40°N, 60°W)

Negative Contributions	U	Positive Contributions
L * L = - 27.13 -H * H = - 12.72 H * -H = - 8.80 I * -I = - 5.57 -L * I = - 2.89 Total -57.11	U1 176.44	L * -L = 89.02 0 * L = 75.57 -L * L = 42.00 -I * I = 19.60 -I * H = 5.31 I * -L = 1.54 ⋮ Total 233.55
	+	
I * -I = - 63.48 I * L = - 50.97 0 * L = - 18.87 -L * L = - 17.99 L * -L = - 12.57 -H * H = - 7.00 L * L = - 2.55 Total -173.43	U2 10.83 + U3 30.09 + U4 - 85.96	L * 0 = 92.04 -I * I = 36.68 H * -I = 34.30 H * -H = 9.73 -I * H = 7.59 -L * I = 3.92 Total 184.26

EUU 58.55 = 131.40 + U5 + E_1 -72.85

Negative Contributions	V	Positive Contributions
0 * L = - 93.28 -H * H = - 9.13 L * L = - 6.12 -I * H = - 5.30 I * -L = - 4.68 -L * I = - 1.22 L * -L = - 0.75 Total - 120.48	V1 - 6.16	L * 0 = 35.70 -L * L = 22.97 I * -I = 22.28 H * -H = 20.01 -I * I = 8.24 H * -I = 5.12 Total 114.32
	+	
-H * H = - 15.18 0 * L = - 14.96 H * -H = - 14.15 -I * I = - 11.25 H * -I = - 8.73 -L * I = - 3.03 L * -L = - 2.20 Total -69.50	V2 -54.06 + V3 82.72 + V4 -39.51	I * -I = 8.04 -L * L = 5.18 L * L = 1.20 -I * H = 0.88 ⋮ Total 15.44

EVV 25.77 = -17.01 + V5 + E_2 42.78

Fig. 4. Linear and nonlinear contributions to the kinetic energy spectra in the low frequency range at 40° N, 60° W, 500 mb, winter 1964.

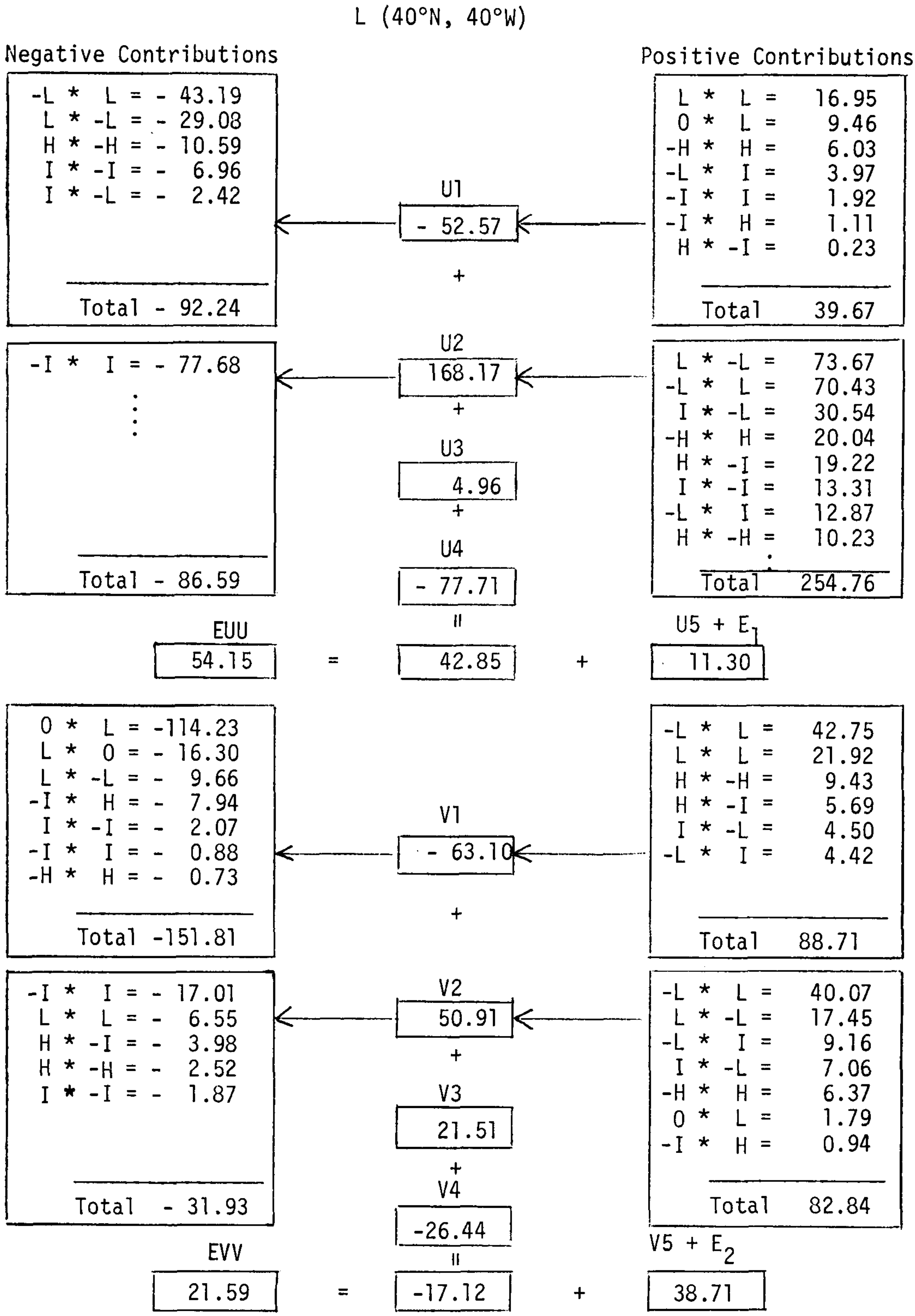

Fig. 5. Linear and nonlinear contributions to the kinetic energy spectra in the low frequency range at 40° N, 40° W, 500 mb, winter 1964.

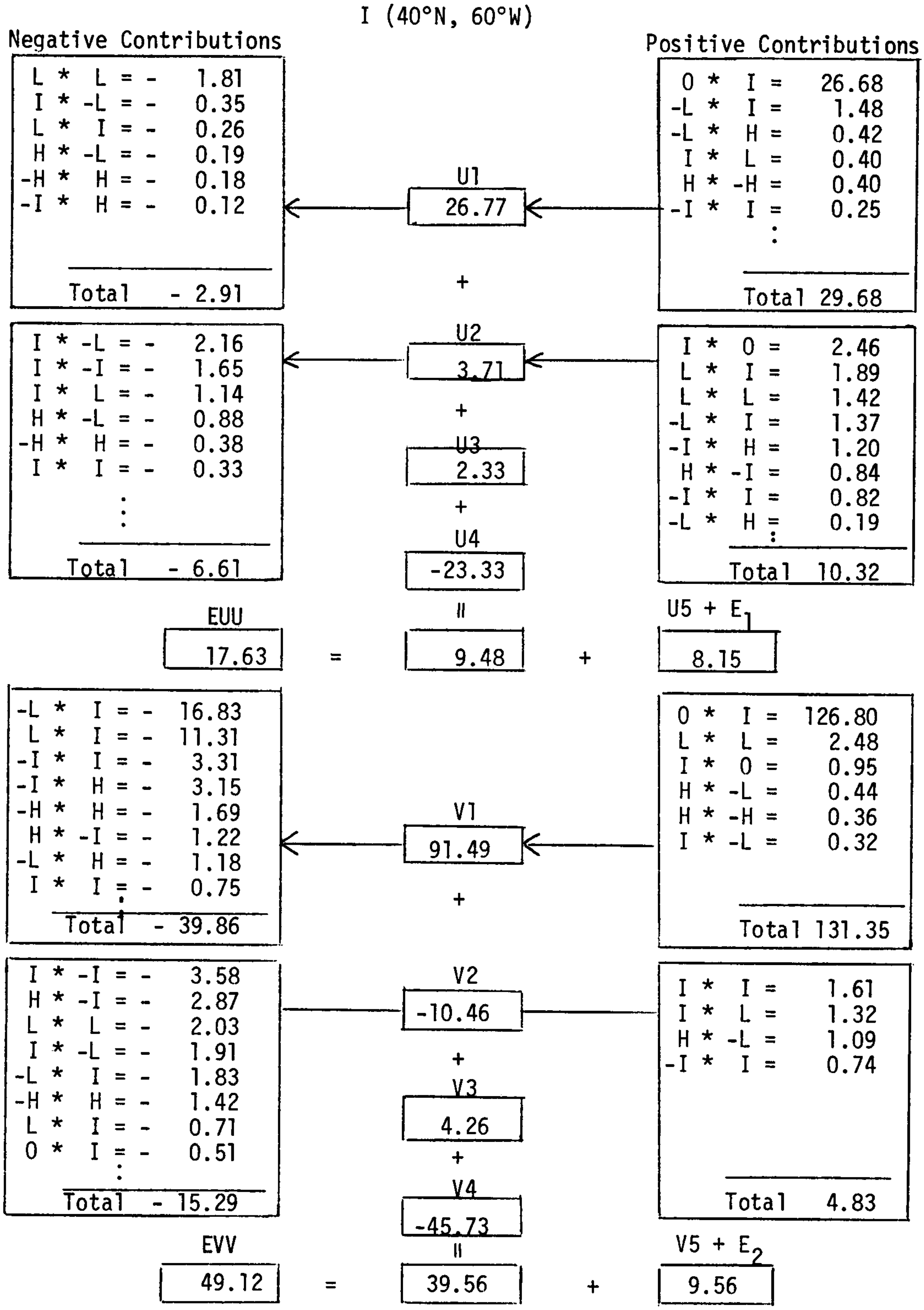

Fig. 6. Linear and nonlinear contributions to the kinetic energy spectra in the intermediate frequency range at 40° N, 60° W, 500 mb, winter 1964.

I (40°N, 40°W)

Negative Contributions	U	Positive Contributions
I * L = - 1.49 -L * I = - 1.30 H * -I = - 0.63 I * I = - 0.31 -H * H = - 0.24 -I * I = - 0.15 H * -L = - 0.10 : Total - 4.22	U1 23.18	0 * I = 22.09 I * -L = 1.90 L * L = 1.57 H * -H = 0.65 I * -I = 0.61 -I * H = 0.37 L * I = 0.21 Total 27.40
	+	
I * -L = - 12.42 -I * I = - 0.98 -H * H = - 0.78 L * I = - 0.55 I * I = - 0.49 0 * I = - 0.35 -I * H = - 0.24 H * -I = - 0.21 : Total -16.10	U2 - 7.22 + U3 0.45 + U4 - 8.61	-L * I = 3.73 I * L = 1.48 H * -H = 1.13 H * -L = 1.11 L * L = 0.78 I * 0 = 0.37 -L * H = 0.28 Total 8.88

EUU				U5 + E_1
17.09	=	7.80	+	9.29

Negative Contributions	V	Positive Contributions
I * L = - 3.97 L * I = - 3.15 -L * H = - 1.61 I * 0 = - 1.36 -I * H = - 0.92 -H * H = - 0.22 : Total - 11.20	V1 67.42	0 * I = 67.93 L * L = 5.71 -L * I = 1.53 H * I = 0.77 I * -L = 0.61 I * I = 0.61 I * I = 0.60 H * -L = 0.52 : Total 78.62
	+	
-L * I = - 3.14 L * L = - 2.66 -H * H = - 1.46 I * L = - 1.34 L * I = - 1.05 0 * I = - 0.94 H * -H = - 0.75 H * -I = - 0.56 : Total - 12.63	V2 - 8.17 + V3 1.54 + V4 - 29.29	I * -L = 1.67 -I * I = 1.45 I * -I = 0.70 H * -L = 0.64 Total 4.46

EVV				V5 + E_2
44.43	=	31.50	+	12.93

Fig. 7. Linear and nonlinear contributions to the kinetic energy spectra in the intermediate frequency range at 40° N, 40° W, 500 mb, winter 1964.

of the interaction terms. The primary interaction combinations, for both U1 and V1, are the interactions between waves of this category and zonal mean motion 0 * I. The ageostrophic terms U4 and V4 serve to counteract the contributions through U1 and V1, respectively. U2 gives small positive contribution, while V2 gives small negative contribution. Both U5 + E_1 and V5 + E_2 give positive contributions. U3 and V3 are small.

(c) *High frequency category, H (Figs. 8 and 9).* Again, the interaction terms U1 and V1 are by far the largest terms and 0 * H are the major interaction combinations for both U1 and V1. U4 and V4 serve to counteract the large positive contributions by U1 and V1, except that V4 at 60°W, 40°N gives positive contributions. Both U5 + E_1 and V5 + E_2 are positive and quite significant.

VI. Spectral structure of atmospheric waves in the region near maximum mean motion (40° N, 60° W)

6.1. *Distributions of the kinetic energy of the mean and turbulent motions*

The distributions of the kinetic energy of the zonal and meridional components of the mean and turbulent motion at 40° N, 0°, 20°, 40°, 60°, 80°, 100°, and 120° W for winter 1964 are shown in Fig. 10. The order of magnitude of the kinetic energy of the maximum mean zonal velocity is about five times that of the zonal and meridional components of the turbulent motion, and is about forty times that of kinetic energy of the mean meridional velocity.

The kinetic energy of the mean zonal motion has a maximum at 40° N and 60° W, where a jet core at 500 mb is located. The kinetic energy of the mean meridional velocity also shows a relative maximum at 40° N and 60° W, with a relative minimum located at 80° W.

The distributions of the kinetic energy of the zonal and meridional components of the turbulent motion are very similar. Both have a relative maximum near 60° W, then remain almost constant toward 0° W. It may be interesting to note that while the kinetic energy of the mean zonal and meridional components of the mean motion decreased from 60° W toward 0° W, the kinetic energy of the turbulent motion remained practically constant over the same region. This fact will be used for the discussion of the energy conversion in the next section.

6.2. *Distributions of the energy spectra in various ranges of frequency*

The distributions of the energy spectra of the zonal and meridional components of the turbulent motion at 40° N in the ranges of high, intermediate, and low frequencies for Winter 1964 are shown in Figs. 11*a* and *b*, respectively. It is seen in Fig. 11*a* that the energy spectrum of the zonal component of the turbulent velocity in the low frequency range shows a minimum at 100° W, then generally increases toward 0° W, whereas the energy spectra of the zonal component of the turbulent velocity in the intermediate and high frequency ranges shows similar distribution with a maximum at 80° W.

It is seen in Fig. 11*b* that the energy spectra of the meridional component of the turbulent motion in the ranges of high and intermediate frequencies show a similar distribution with a maximum at 60° W, whereas the spectrum of that in the low frequency shows a minimum at 80° W, then increases toward 0° W with a relative maximum at 60° W.

It may be interesting to note that the energy spectra of the zonal and meridional components of the turbulent motion in the high and intermediate frequency ranges decrease from 60° W to 0° W, whereas those in the low frequency range increase in the same region. Yet, the total kinetic energy of the turbulent motion remains practically constant in the same region as shown in Fig. 11. This suggests that a transfer of kinetic energy of the turbulent motion from the high and intermediate frequency ranges to the low frequency range may occur in the region between 60° and 0° W. One may, therefore, infer that as waves travel eastward from the center of maximum kinetic energy of mean motion, the amplitude of the long waves grows at the expense of energy of the short waves. Further discussions will be made on this point in the next two sections on the contributions of nonlinear interactions. The growth of intermediate and high frequency waves agrees with the instability theory on the amplifying baroclinic waves between 80° and 60° W and damping barotropic waves from 60° W eastward (Phillips, 1954).

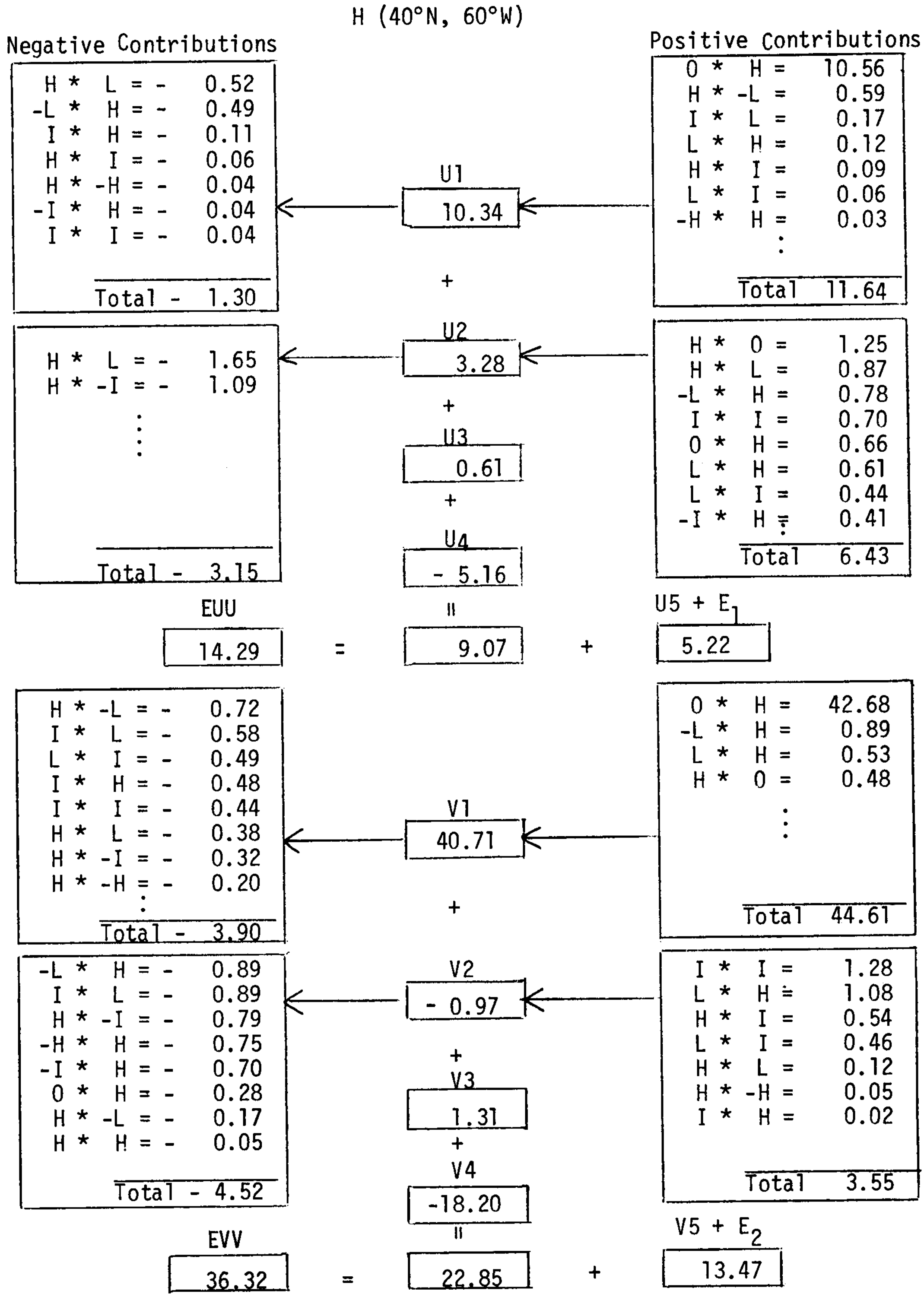

Fig. 8. Linear and nonlinear contributions to the kinetic energy spectra in the high frequency range at 40° N, 60° W, 500 mb, winter 1964.

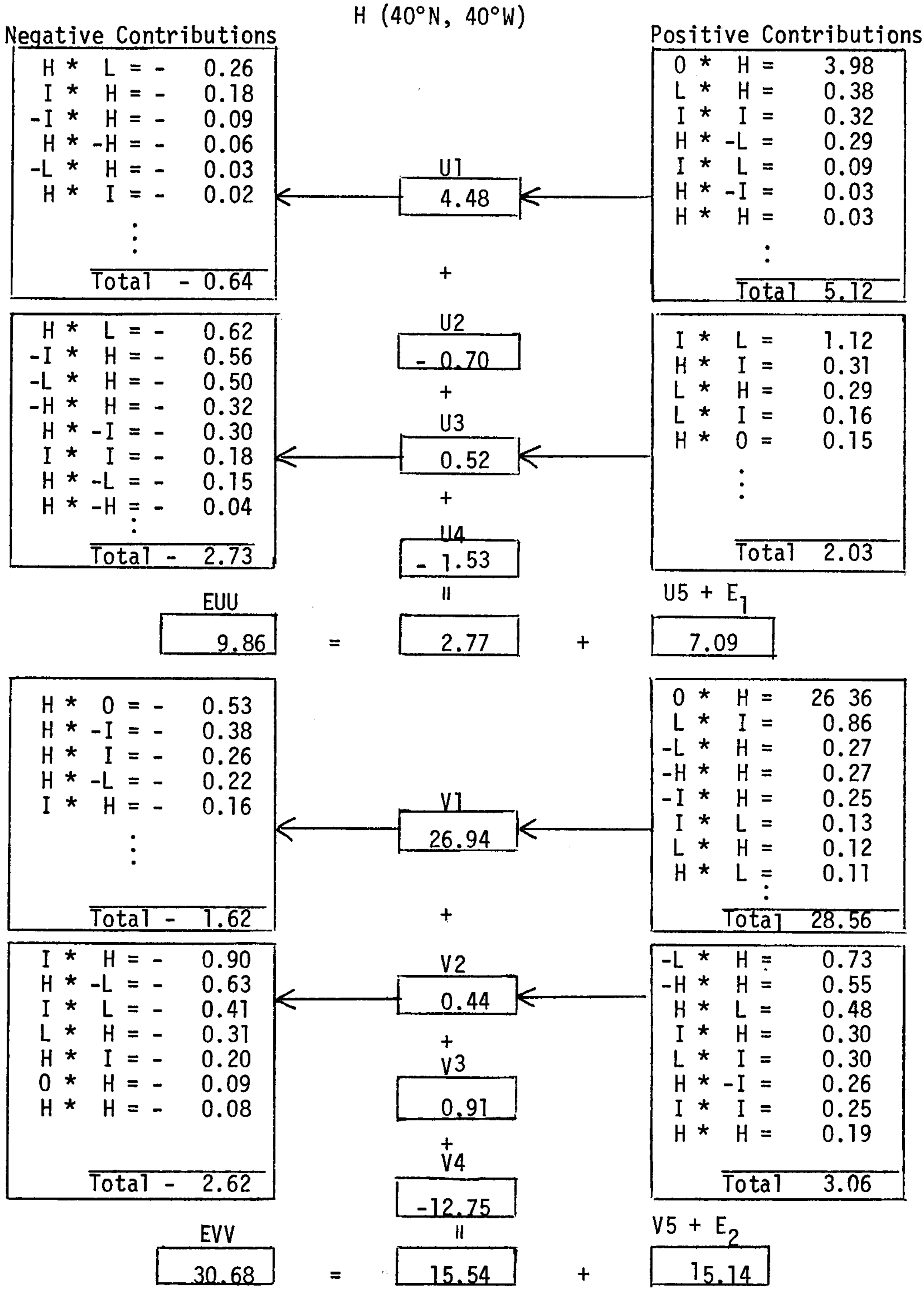

Fig. 9. Linear and nonlinear contributions to the kinetic energy spectra in the high frequency range at 40° N, 40° W, 500 mb, winter 1964.

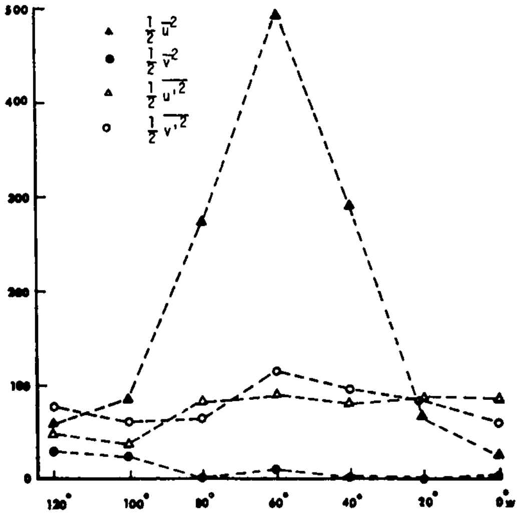

Fig. 10. Kinetic energy distribution on 40° N, 500 mb, in winter 1964. They are in the unit of 10^4 cm^2 sec^{-2}.

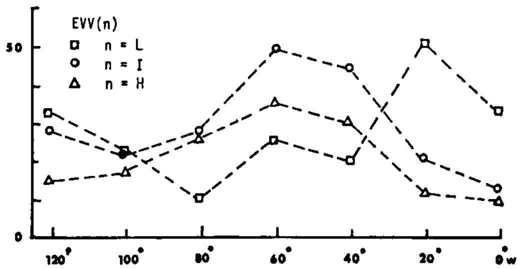

Fig. 11b. The distributions of energy spectra for meridional component of turbulent motion, EVV(n), in 10^4 cm^2 sec^{-2}, on 40° N, 500 mb, winter 1964.

6.3. *Contributions of the nonlinear interactions to the energy spectra of the zonal component of the turbulent motion*

The distributions of the contributions of the nonlinear interactions, among waves of various frequency ranges, to the energy spectra of the zonal component of the turbulent motion are shown in Figs. 12*a*, 13*a*, and 14*a*. For convenience of discussion, only the spectral values of the interaction between the mean zonal motion and waves of various frequency ranges, denoted by (0 * L), (0 * I). (0 * H), and the spectral values of the difference between the energy spectra in a certain frequency range and interaction between the mean zonal motion and waves of that frequency range, denoted by U1 (H) − $(0 * H)_1$, U2 (L) − $(0 * L)_2$, etc., are shown in Figs. 12*a*, 13*a*, and 14*a*. The subscripts, 1 and 2, refer to the terms U1 and U2 respectively.

It is seen from Figs. 12*a*, 13*a*, and 14*a* that in the region from 80° W to 20° W, the order of magnitude of U1 is generally greater than that of U2, except for U2 (L) − $(0 * L)_2$ which has energy greater than that of U1 (L) at 40° and 20° W. It may be noted that interactions, $(0 * L)_1$, $(0 * I)_1$, $(0 * H)_1$ and U1 (L) − $(0 * L)_1$, have their maxima located between 60° and 80° W, whereas U2 (L) − $(0 * L)_2$ shows its maximum at 40° and 20° W. The interactions U2 (L) − $(0 * L)_2$ give secondary contributions at 80° W and U1 (L) − $(0 * L)_1$ at 20° and 0° W. Interactions of other categories are small and may be neglected.

Comparing the distributions of the contributions of the nonlinear interactions with the distributions of energy spectra, one may infer

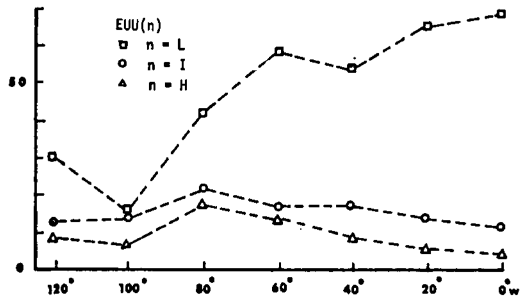

Fig. 11a. The distributions of energy spectra for zonal component of turbulent motion, EUU(n), in 10^4 cm^2 sec^{-2}, on 40° N, 500 mb, winter 1964.

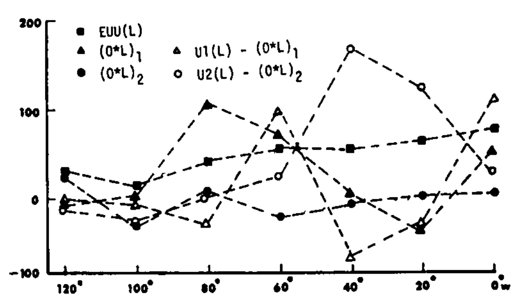

Fig. 12a. The distributions of the contributions of the nonlinear interactions to the kinetic energy spectra of zonal component of turbulent motion in low frequency range for 40° N, 500 mb, winter 1964. (Unit in 10^4 cm^2 sec^{-2}.)

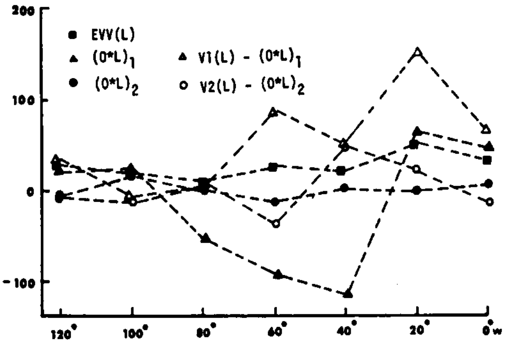

Fig. 12b. The distributions of the contributions of nonlinear interactions to the kinetic energy spectra of meridional component of turbulent motion in low frequency range for 40° N, 500 mb, winter 1964. (Unit in 10^4 cm^2 sec^{-2}.)

that the mechanism for the distribution of the kinetic energy of the zonal component of the turbulent motion in the high and intermediate frequency ranges is essentially due to interactions of the mean motion and waves of high and intermediate frequencies, respectively. However, the mechanism for the distribution of the kinetic energy of the zonal component of the turbulent motion in the low frequency range in the region from 60° to 0° W is due to the interactions of U1 (L) − (0 * L) and U2 (L) − $(0 * L)_2$, i.e., contributions from interactions of motion in various frequency ranges. These results further illustrate that the long waves grow at the expense of energy of the short waves as they travel eastward from the center of maximum kinetic energy of mean motion. A detailed account of the interactions may be found in the diagrams of linear and nonlinear interactions.

6.4. *Contributions of nonlinear interactions to the energy spectra of the meridional component of the turbulent motion*

The distributions of the contributions of the nonlinear interactions among waves of various frequency ranges to the energy spectra of the meridional component of the turbulent motion are shown in Figs. 12*b*, 13*b*, and 14*b*. It is seen from these three figures that the order of magnitude of V1 is generally greater than that of V_2 except for V2 (L) − $(0*L)_2$ which has energy comparable to that of V1. It may be noted that the interactions, V1 (L) − $(0 * L)_1$, $(0 * I)_1$ and $(0 * H)_1$, show their maxima at 60° W, whereas $(0 * L)_1$ and V1 (I) − $(0 * I)_1$ show their minima between 40° and 60° W.

Comparing the distributions of the contributions of the nonlinear interactions with the distributions of energy spectra, one may infer that the mechanism for the distributions of the kinetic energy of the meridional component of the turbulent motion in the intermediate and high frequency ranges is essentiaaly due to the interactions $(0 * I)_1$ and $(0 * H)_1$, respectively, whereas that in the low frequency range from 60° to 0° W is essentially due to the contribution of the interactions V1 (L) − $(0 * L)_1$ and V2 (L) − $(0 * L)_2$. This indicates that the kinetic energy of the meridional component of the turbulent motion in the high and intermediate frequency ranges is primarily associated with the mean motion, whereas that in the low frequency range does not associate with the mean motion. The fact that the kinetic energy of the low frequency waves does not associate with the mean motion and that it increases as waves travel eastward, as shown in Fig. 11*b*, indicates that the growth of the kinetic energy of the low frequency waves

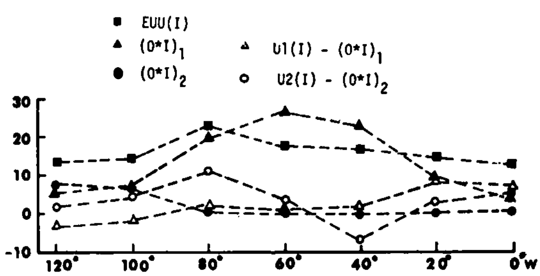

Fig 13a. The distributions of the contributions of the nonlinear interactions to the kinetic energy spectra of zonal component of turbulent motion in intermediate frequency range for 40° N, 500 mb, winter 1964. (Unit in 10^4 cm^2 sec^{-2}.)

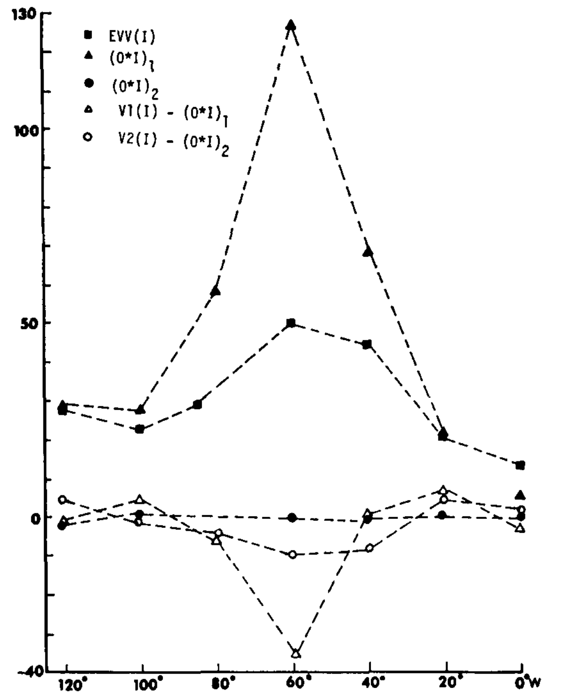

Fig. 13b. The distributions of the contributions of the nonlinear interactions to the kinetic energy spectra of meridional component of turbulent motion in intermediate frequency range for 40° N, 500 mb, winter 1964. (Unit in 10^4 cm^2 sec^{-2}.)

is at the expense of the kinetic energy of waves of higher frequencies.

VII. Summary and conclusions

In the investigation of the spectral structure of atmospheric waves near the center of maximum mean motion, it is found that interactions of waves of low frequencies (L * −L, −L * L, and L * L) and between zonal mean motion and waves of low frequency contribute most to the zonal energy spectrum in low frequency range. However, interactions between zonal mean motion and waves of frequency range in question contribute most to the zonal energy spectra in intermediate and high frequency

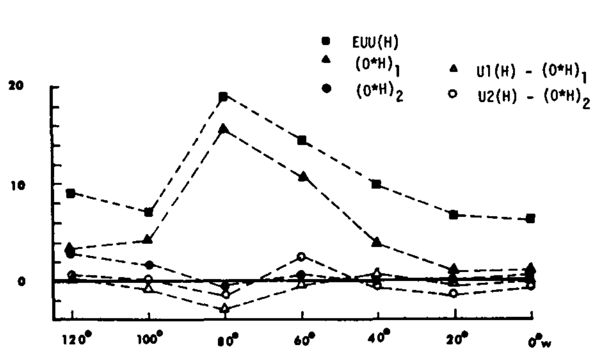

Fig. 14a. The distributions of the contributions ofthe nonlinear interactions to thekinetic energy spectra of zonal component of turbulent motion in high frequency range for 40° N, 500 mb, winter 1964. (Unit in 10^4 cm^2 sec^{-2}.)

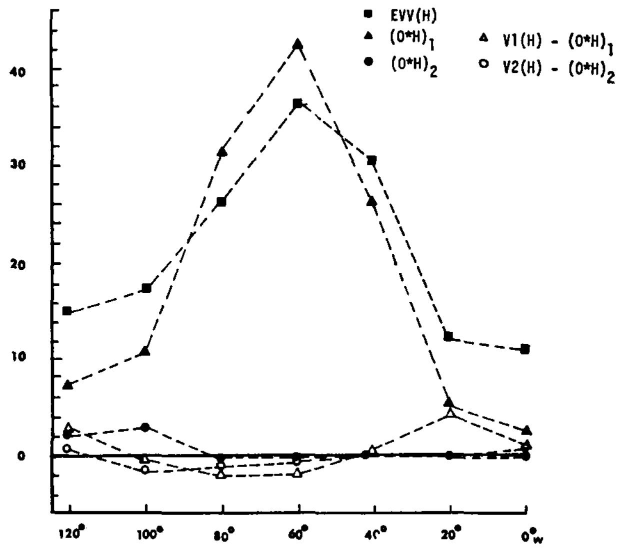

Fig. 14b. The distributions of the contributions of the nonlinear interactions to the kinetic energy spectra of meridional component of turbulent motion in high frequency range for 40° N, 500 mb, winter 1964. (Unit in 10^4 cm^2 sec^{-2}.)

ranges. The geostrophic term (U4) serves to counteract the positive contributions by the nonlinear interactions. The sphericity term (V3) and Reynolds stress plus error term (V5 + E_2) are the major contributions to the meridional component of kinetic energy in low frequency range, while the nonlinear interaction term arising from the zonal transport of meridional kinetic energy (V1) is the largest term contributing to the kinetic energy of the meridional velocity in the intermediate and high frequency ranges. The nonlinear interactions involving the zonal mean motion and the waves of frequency range in question have large contributions to the meridional kinetic energy in intermediate and high frequency ranges. However, it serves to abstract the energy in low frequency range.

It is found that the kinetic energy of turbulent motion to the east of maximum mean motion of the quasi-stationary polar-front jet stream remains constant and is greater than that to the west of it. It is also found that as waves travel eastward from the center of maximum mean zonal motion, the velocity-amplitudes of waves of low frequencies grow at the expense of the kinetic energy of waves of higher frequencies. This suggests that the center of maximum mean motion of the jet stream tends to excite wave motion of high frequencies and that the kinetic energy of these waves is transferred to waves of lower frequencies through nonlinear interactions as waves travel eastward.

Appendix a. Interpretation of nonlinear interactions

Let two waves, q and p, be expressed by

$$q = A \cos k(t - t_1), \quad p = B \cos j(t - t_2), \quad k > j$$

where A and B are the wave amplitudes, k and j are the frequencies, and t_1 and t_2 are phases of the waves.

Furthermore, let Q and P be the Fourier transform of q and p respectively. Thus, by (2-1)

$$Q_r(k) = \tfrac{1}{2} A \cos kt_1 \quad Q_i(k) = -\tfrac{1}{2} A \sin kt_1$$

$$P_r(j) = \tfrac{1}{2} B \cos jt_2 \quad P_i(j) = -\tfrac{1}{2} B \sin jt_2$$

where

$$Q(k) = Q_r(k) + i\, Q_i(k) \quad P(j) = P_r(j) + i\, P_i(j)$$

Since

$$\begin{aligned} q\,p &= A\ B \cos k(t-t_1) \cos j(t-t_2) \\ &= 2[Q_r(k)P_r(j) - Q_i(k)P_i(j)] \cos (k+j)t \\ &\quad - 2[Q_i(k)P_r(j) + Q_r(k)P_i(j)] \sin (k+j)t \\ &\quad + 2[Q_r(k)P_r(j) + Q_i(k)P_i(j)] \cos (k-j)t \\ &\quad - 2[Q_i(k)P_r(j) - Q_r(k)P_i(j)] \sin (k-j)t \end{aligned}$$

the interaction of waves q and p with frequencies k and j will result in two waves with frequencies $(k+j)$ and $(k-j)$. The wave with frequency $(k+j)$ has its complex amplitude (2-1)

$$[Q_r(k)P_r(j) - Q_i(k)P_i(j)] + i[Q_i(k)P_r(j) + Q_r(k)P_i(j)] = Q(k)P(j)$$

whereas the wave with frequency $(k-j)$ as its complex amplitude (2-1)

$$[Q_r(k)P_r(j) + Q_i(k)P_i(j)] + i[Q_i(k)P_r(j) - Q_r(k) P_r(j)] = Q(k)P(-j).$$

REFERENCES

Barrett, E. W. 1961. Some applications of harmonic analysis to the study of the general circulation. I. Harmonic analysis of some daily and five-day mean hemispheric contour charts. *Beitr. Phys. Atmos 33*, 280–332.

Barrett, E. W. 1961. Some applications of harmonic analysis to the study of the general circulation. II. Calculations of some product-spectra and related quantities. *Beitr. Phys. Atmos. 33*, 333–355.

Benton, G. S. & Kahn, A. B. 1958. Spectra of large-scale atmospheric flow at 300 millibars. *J. Meteor. 15*, 404–410.

Charney, J. G. 1948. On the scale of atmospheric motions. *Geof. Publ. 17*, No. 2.

Chiu, W.-C. 1961. The energy equation of atmospheric motions in the frequency domain. *Scientific Report No. 2*, AF 19(607)-6146. Dept. of Meteor. and Ocean., New York University.

Chiu, W.-C. 1968. The energy equation of atmospheric motions in the frequency domain. *NCAR MS-68-86*, National Center for Atmospheric Research.

Eliasen, E. 1958. A study of the long atmospheric waves on the basis of zonal harmoic analysis. *Tellus 10*, 206–215.

Eliasen, E. & Machenhauer, B. 1965. A study of the fluctuations of the atmospheric planetary patterns represented by spherical harmonics. *Tellus 17*, 220–238.

Eliasen, E. & Machenhauer, B. 1969. On the observed large-scale atmospheric wave motion. *Tellus 21*, 149–166.

Estoque, M. A. 1955. The spectrum of large-scale turbulent transfer of momentum and heat. *Tellus 7*, 177–185.

Goertzel, G. 1958. An algorithm for the evaluation of finite, trigonometric series. *Amer. Math Monthly 65*, 34–35.

Lilly, D. K. 1972. Wave momentum flux—a GARP problem. *Bull. Amer. Meteor. Soc. 53*, 17–23.

Lipps, F. B. 1963. Stability of jets in a divergent barotropic fluid. *J. Atmos Sci. 20*, 120–129.

Kao, S.-K. 1954. An analysis of the longitudinal spectrum of the large-scale atmospheric motion. *Bull. Amer. Meteor. Soc. 35*, 84.

Kao, S.-K. 1962. Large-scale turbulent diffusion in a rotating fluid with applications to the atmosphere. *J. Geophys. Res. 67*, 2347–2359.

Kao, S.-K. 1965. Some aspects of the large-scale turbulence and diffusion in the atmosphere. *Quart. J. Roy. Meteor. Soc. 91*, 10–17.

Kao, S.-K. 1965. On the spectrum of geostrophic winds. *Quart. J. Roy. Meteor. Soc. 91*, 338.

Kao, S.-K., 1968. Large-scale atmospheric motion and transports in frequency wave-number space. *J. Atmos. Sci. 25*, 32–38.

Kao, S.-K. & Bullock, W. S. 1964. Lagrangian and Eulerian correlations and energy spectra of geostrophic velocities. *Quart. J. Roy. Meteor. Soc. 90*, 166–174.

Kao, S.-K. & Gain, A. A. 1968. Large-scale dispersion of clusters of particles in the atmosphere. *J. Atmos. Sci. 25*, 214–221.

Kao, S.-K. & Henderson, D. 1970. Large-scale dispersion of clusters of particles in various flow patterns. *J. Geophys. Res. 75*, 3104–3113.

Kao, S.-K. & Hurley, W. P. 1962. Variations of the kinetic energy of large-scale eddy currents in relation to the jet stream. *J. Geophys. Res. 67*, 4233–4242.

Kao, S.-K. & Powell, D. C. 1969. Large-scale dispersion of clusters of particles in the atmosphere. II. Stratosphere. *J. Atmos. Sci. 26*, 734–740.

Kao, S.-K. & Sagendorf, J. 1970. The large-scale meridional transport of sensible heat in wavenumber frequency. *Tellus 22*, 172–185.

Kao, S.-K., Tsay, C.-Y. & Wendell, L. L. 1970. The meridional transport of angular momentum in wavenumber frequency space. *J. Atmos. Sci. 27*, 614–626.

Kao, S.-K. & Wendell, L. L. 1970. The kinetic energy of the large-scale atmospheric motion in wavenumber frequency space. I. Northern Hemisphere. *J. Atmos. Sci. 27*, 359–375.

Kuo, H.-L. 1951. Vorticity transfer as related to the development of the general circulation. *J. Meteor. 8*, 307–315.

Phillips, N. A. 1954. Energy transformations and meridional circulations associated with simple baroclinic waves in a two-level, quasi-geostrophic model. *Tellus 6*, 273–286.

Phillips, N. A. 1963. Geostrophic motion. *Rev. Geophys. 1*, 123–176.

Saltzman, B. 1958. Some hemispheric spectral statistics. *J. Meteor.* *15*, 259–263.

Saltzman, B. & Fleisher, A. 1962. Spectral statistics of the wind at 500 mb. *J. Atmos. Sci.* *19*, 195–204.

Tsay, C. Y. 1972. An investigation of the spectral structure of waves in middle latitudes. Ph.D. Thesis, 135 pp., University of Utah, Salt Lake City, Utah.

Van der Hoven, I. 1957. Power spectrum of horizontal wind speed in the frequency range from 0.0007 to 900 cycles per hour. *J. Meteor.* *14*, 160–164.

Van Mieghem, J. 1961. Zonal harmonic analysis of the Northern Hemisphere geostrophic wind field. *I.U.G.G. Monogr.*, No. 8, p. 57. Paris.

ИССЛЕДОВАНИЕ СПЕКТРАЛЬНОЙ СТРУКТУРЫ АТМОСФЕРНЫХ ВОЛН ВБЛИЗИ СТРУЙНОГО ТЕЧЕНИЯ

Исследование нелинейных взаимодействий вблизи центра максимума средней скорости струйного течения указывает, что взаимодействия волн низких частот между собой и со средним зональным потоком дают наибольший вклад в низкочастотную часть спектра энергии зональной компоненты турбулентного движения, в то время как эффекты сферичности и напряжения Рейнольдса дают наибольший вклад в низкочастотную часть спектров мериодиональной компоненты турбулентного движения. В интервалах промежуточных и высоких частот взаимодействия между средним зональным движением и волнами рассматриваемых частот дают наибольший вклад в соответствующие спектры. При исследовании спектральной структуры атмосферных волн вблизи струйного течения найдено, что в области максимального зонального среднего движения кинетическая энергия зональной и меридиональной компонент турбулентного движения обычно поддерживается нелинейными взаимодействиями между волнами разных частот и зональным потоком. Найдено также, что по мере распространения волн на восток от центра максимума среднего зонального потока амплитуды скорости волн низких частот растут за счет кинетической энергии волн более высоких частот. Отсюда можно сделать вывод, что центральная часть струйного течения стремится возбудить волновое движение высоких частот и что кинетическая энергия этих волн посредством нелинейных взаимодействий переносится к волнам более низких частот.